EB2014-SA-019

COUPLED CFD AND FE THERMAL MECHANICAL SIMULATION OF DISC BRAKE

[1]Tang, Jinghan*; [1]Bryant, David; [1]Qi, Hongsheng
[1]University of Bradford, United Kingdom

KEYWORDS –finite element, computational fluid dynamics, disc brake, co-simulation, conjugate heat transfer

ABSTRACT – To achieve a better solution of disc brake heat transfer problem under heavy duty applications, the accurate prediction of transient field of heat transfer coefficient is significant. Therefore, an appropriate coupling mechanism between flow field and temperature field is important to be considered. In this paper, a transient conjugate heat transfer co-simulation disc brake model has been presented in order to improve the accuracy and feasibility of conventional coupled FE and CFD method. To illustrate the possible utilizations of this co-simulation method, a parameter study has been performed e.g. geometric, material, and braking application. The results show the advantage of the co-simulation method in terms of computing time efficiency and accuracy for solving complex braking heat transfer problem.

1 INTRODUCTION

The numerical thermal analysis is very significant to the design of disc brake especially for heavy duty brake applications which can cause severe thermal effects. According to (1), the convective heat dissipation is a main cooling mechanism for disc brake especially for the ventilated disc. A well-known problem of brake thermal analysis is that the convective heat dissipation of a ventilated disc during the heavy duty condition is complicated, thus it is difficult to determine the convective heat transfer coefficient (HTC) distribution which is important in heat transfer calculation according to Newton's cooling law.

Nowadays, computational fluid dynamics (CFD) techniques have been widely used in brake research in order to improve the cooling performance of brake design and the prediction of HTC distribution. The coupling approach between finite element (FE) solid heat conduction and CFD fluid heat transfer has been investigated by several researchers. In 2010, Pevec *et al* (2) obtained the HTC distribution under different temperature and velocity using a steady-state CFD solver and converted it into the input file of FE model as a surface film condition. Belhocine *et al* (3) performed a transient CFD simulation and determined the area-weighted average HTC variation with time on each surface of a ventilated disc. The data therefore was imported into the FE model as a surface film condition. The comparison of these two approaches implies that (2) enabled better HTC distribution i.e. data mapping between FE and CFD codes. Whilst (3) achieved transient HTC which can improve the cooling performance prediction in more complicated braking applications.

To achieve the advantages of both of the coupling approaches above, a transient conjugate heat transfer co-simulation model of repetitive brake has been performed by the authors. As presented previously in (4), the coupling between CFD and FE codes is enabled using a third party data exchanging interface. The two codes run simultaneously and data exchanging performed at each time increments. The results have demonstrated the accuracy and efficiency of the co-simulation method in both flow field and temperature field.

This paper initially reviewed the method used in (4) and then extends the model by parameter modifications to illustrate the possibility, utility, and advantages of the co-simulation method.

2 MODEL SETUP

Initially, the co-simulation methodology in (4) will be introduced. To validate the results of the co-simulation method, (4) performed a comparison with the numerical and experimental results in (2). Therefore, the basic setup, for instance, the geometry, material, braking application are identical with (2). However, it should be noted that more details of model setup and results validation can be seen in (4).

2.1 Co-simulation Setup

The data exchanging process is demonstrated by figure 1. The two codes run simultaneously and exchange data at each time increment. To enable the data exchanging between the CFD and FE codes, the third party interface MpCCI was used. There were three conditions which had to be satisfied:

1. The two codes should have identical unit system (SI was used).
2. The coupling surfaces in the two models should have the same geometry.
3. The two codes should have the same fixed time increment size ($\Delta t = 0.1s$).

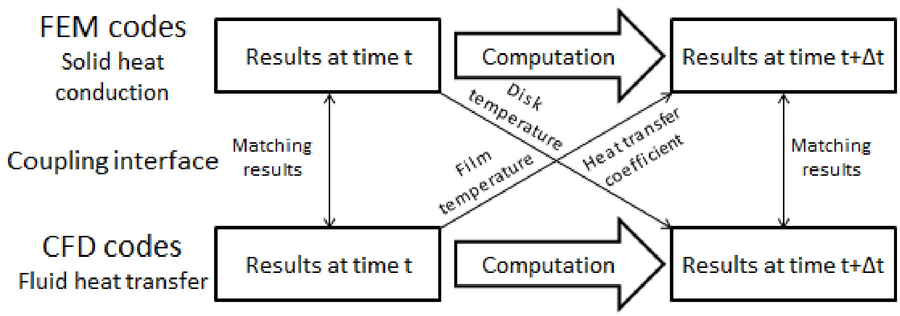

Figure 1: The two way coupling data exchange (4)

2.2 FEM model

In this study, a 3D axisymmetric segment of an EN-GJL-250 grey cast iron ventilated disc brake with 41 vanes following an AMS (As shown in figure 2) test procedure has modelled. Table 1 and 2 provided the material property and vehicle data for the analytical calculation in this study. It is assumed that the initial disc temperature was uniformly 100 ℃ and the ambient air temperature was 30 ℃ during the braking operation. The thermal load was assumed to be uniformly applied on the rubbing surface shown in figure 1 and the heat flux was calculated according to the brake application and equation adopted from (1):

$$q(t) = \frac{(1-t/t_{stop})*m_{vehicle}*|a|*d_{f/r}*v_{init}*\eta_{disc}}{4*\pi*(r_o^2-r_i^2)} \qquad \text{(Equation 1)}$$

where q(t) is the heat flux and t_{stop} is the vehicle stopping time. The other notations in Equation 1 and data used are provided in Tables 1 and 2.

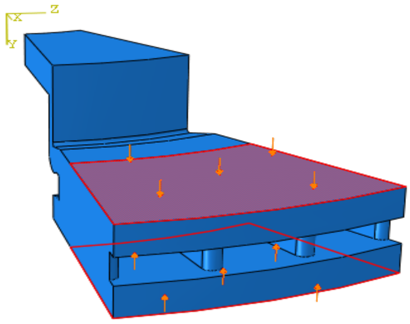

Figure 1: Finite element model

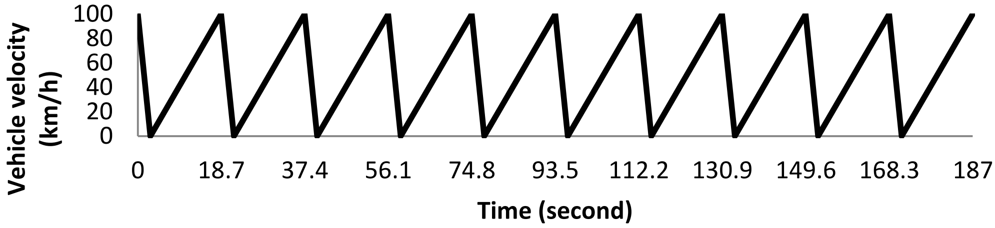

Figure 2: vehicle velocity time courses

Nomenclature and units	Value
Vehicle mass $-m_{vehicle}$ (Kg)	1760
Initial speed $-v_{init}$ (km/h)	100
Acceleration $-a_c$ (m/s^2)	1.73
Deceleration $-a$ (m/s^2)	9.8
Brake distribution for front $-d_{f/r}$ (%)	76
Outer friction radius of pad $-r_o$ (mm)	139
Inner friction radius of pad $-r_i$ (mm)	93.5
Share of absorbed heat by disc $-\eta_{disc}$ (%)	99

Table 1: Vehicle data and braking data (2)

Grey cast irons	Material designation				
	Unit	EN-GJL-200	EN-GJL-250	EN-GJL-300	EN-GJL-350
Density-ρ	Kg/m^3	7150	7200	7250	7300
Elastic module-E	MPa	88000	103000	108000	123000
Poisson's ratio-ν	-	0.26	0.26	0.26	0.26
Specific heat-C_p	J/kgK	535	535	535	535
Thermal conductivity-λ					
At 100°C	W/mK	50	48.5	47.5	45.5
At 200°C		49	47.5	46	44.5
At 300°C		48	46.5	45	43.5
At 400°C		47	45	44	42
At 500°C		46	44.5	43	41.5

Table 2: Material data for the grey cast iron disc (5)

2.3 CFD model

The flow field boundary conditions setup was adopted from (2, 4 and 6) and is illustrated by figure 3. RNG k-ε (k-epsilon) viscosity model was selected to describe the turbulences. The surface roughness height was taken at 0.01mm (3). To control the transient rotation velocity variation of disc due to repetitive brake applications, user defined function codes were written.

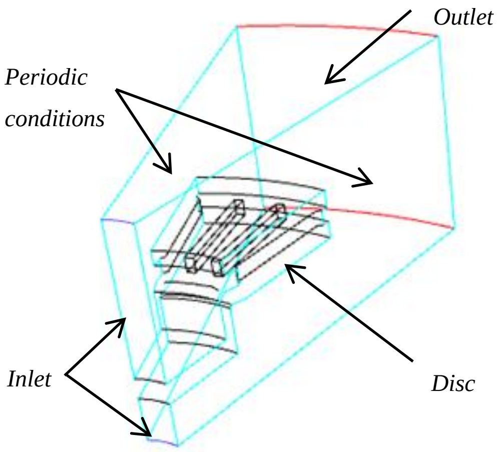

Figure 3: CFD model flow field geometry and boundary conditions

3 RESULTS

Figure 4 shows the variation of heat transfer coefficient in one of the 10 brake applications, it implies that the co-simulation method has the same capability in transient HTC prediction as the method used by (3). For the temperature prediction, figure 5 presents the maximum temperature evolution of the disc and comparing with the result in (2). It illustrates that the co-simulation method has the capability to provide accurate temperature field prediction in the heavy duty brake application simulation. More results and discussion of the AMS test simulation can be founded in (4).

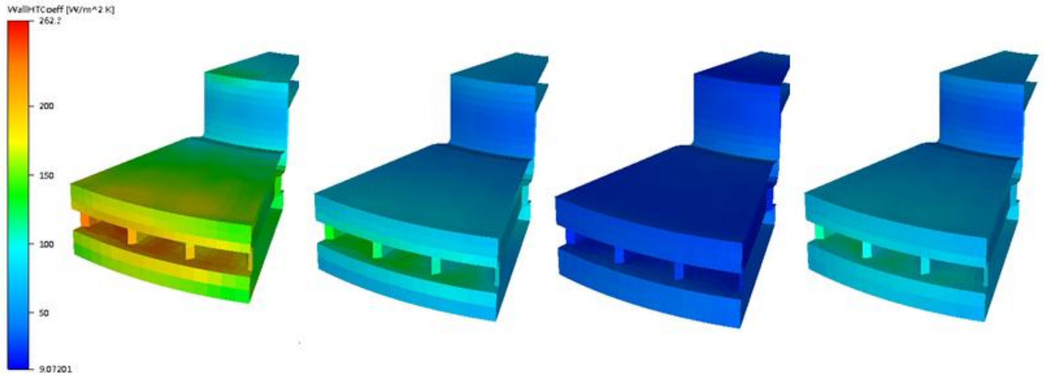

Figure 4 Heat transfer coefficient distribution variation in a single brake application

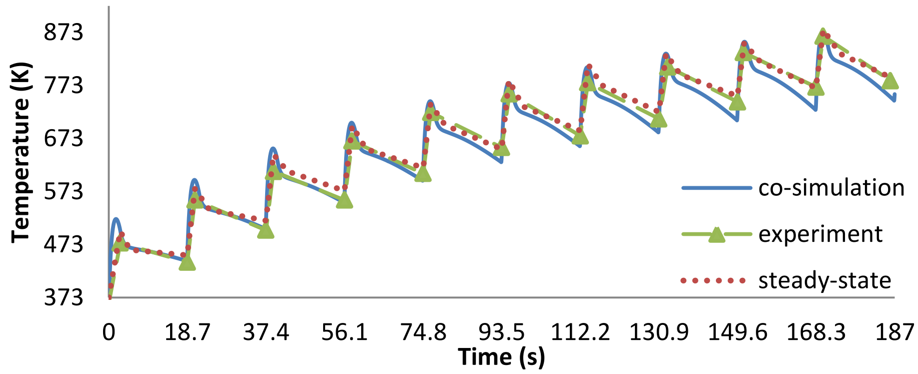

Figure 5 Maximum disc temperature evolution comparisons

4 PARAMETER STUDY

To give better understanding of the temperature prediction capability of the co-simulation method, the effects of modelling parameters have been investigated and discussed including mesh sensitivity, material properties, geometry, and braking application.

4.1 Influence of meshing

To investigate the coupling compatibility, computational time efficiency and temperature prediction results of the co-simulation method for different meshes, both the FEM and CFD models have been meshed in three densities, and the 9 possible co-simulation combinations have been tested and shown in table 3.

In table 3, it is found that for the FE model sector, the maximum temperature increases with coarser meshing. However, the CFD model meshes do not have significant influence i.e. the CFD model is relatively not sensitive to mesh. Regarding the computing time efficiency, it shows that both FEM and CFD models increase linearly with the meshing density refining. In addition, the co-simulation computing time approximately equals the sum of FEM and CFD computing time which reveals the data exchanging almost spent no extra computing resources.

FEM model / CFD model	Element size, element quantity and time		
	2mm	3.3mm	5mm
	76438	19399	6675
	10min	2min	30s
Element size, Element quantity and time	**Maximum temperature (K) at the end of 10 brake applications and computing time**		
2mm 703607 102min	782.9 (111min)	799.3 (108min)	811.8 (107min)
3.3mm 166277 22min	780.5 (28min)	799.1 (25min)	811.8 (23min)
5mm 40405 4min30s	782.8 (14min)	798.8 (7min30s)	812.6 (6min)

Table 3 Co-simulation element size, element quantity, maximum temperature and computational time comparison matrix

4.2 Influence of disc materials

To investigate the influence of material to the temperature field prediction, four types of grey cast irons have been applied in this study including EN-GJL-200, EN-GJL-250, EN-GJL-300 and EN-GJL-350. The temperature dependent material properties were provided by table 2.

The peak temperature results for the different materials at 171s and 187s (i.e. end of heating phase and end of cooling phase) show an increasing trend with the increasing of density or decreasing conductivity of cast irons. However, the increments were small (1.1 ℃ to 4 ℃) which implies that the selected materials have only small effects.

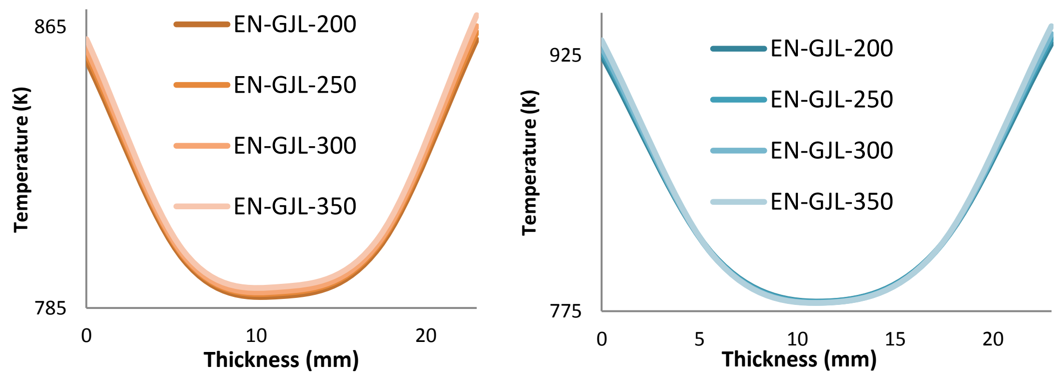

Figure 6 Temperature varying with thickness for different materials at 171s and 187s

For the temperature distribution, figure 6 illustrated the temperature along the disc thickness at 171s and 187s. In general, the temperature distributions for different materials have similar shape and slope. There is an approximately 60 ℃ temperature decrease in the middle plane of the disc at 171s. However, at 187s the curves present that the temperature decrease is over 100 ℃ and the lower the thermal conductivity of the material, the sharper the temperature decreased through the thickness. This phenomenon has also been identified by (3).

4.3 Influence of disc geometry

In the aspect of geometry, both solid and ventilated discs have been modelled. The solid disc was modelled with identical geometry to that of the ventilated disc but with a total thickness of 16mm; this equated to the combined friction ring thickness of the ventilated disc.

Figure 7 shows the maximum temperature evolution curves for the solid and ventilated discs in both the heat insulation condition and co-simulation condition. In the heat insulation condition, the temperature difference between the solid and ventilated disc at the end of 10th brake application was 56.2 ℃. In the co-simulation condition, the temperature difference was 81.2 ℃ which is 145% of the solid disc case. Obviously, the ventilated disc showed a significant advantage from the cooling effect due to the increased ‘wetted’ area.

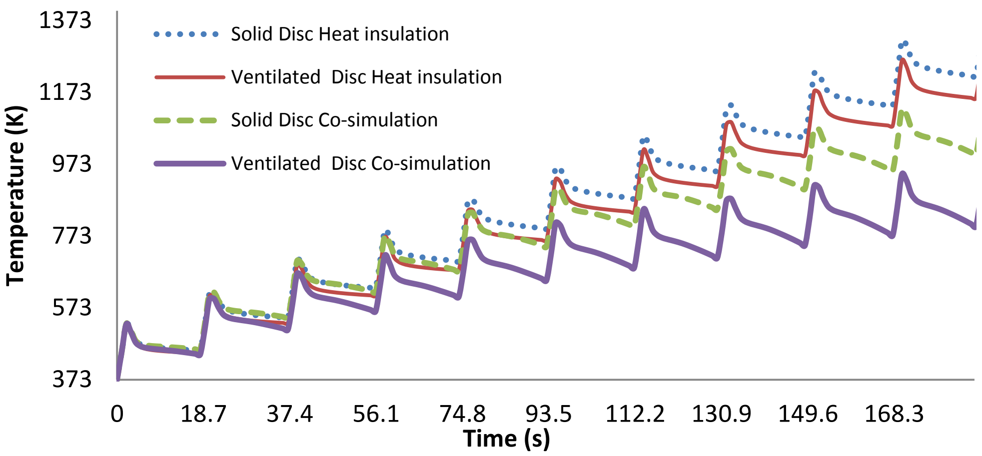

Figure 7 Temperature evolution curves of solid and ventilated discs

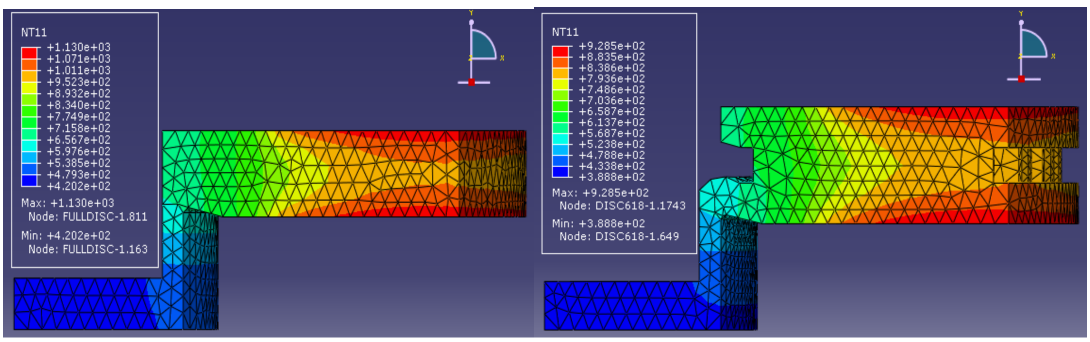

Figure 8 Temperature varying with thickness for different geometry at 171s

The temperature variation through the disc thickness for solid and ventilated discs at 171s is shown in figure 8. It illustrates that the maximum temperature of the solid disc was higher than that of the ventilated one. Furthermore, the temperature distribution for the friction ring section (inboard and outboard) of discs, the ventilated disc was similar to that of the solid. In summary, it reveals that whilst the ventilated disc can provide better cooling performance is also and maintains similar temperature distribution characteristics to that of a solid disc.

4.4 Influence of braking operations

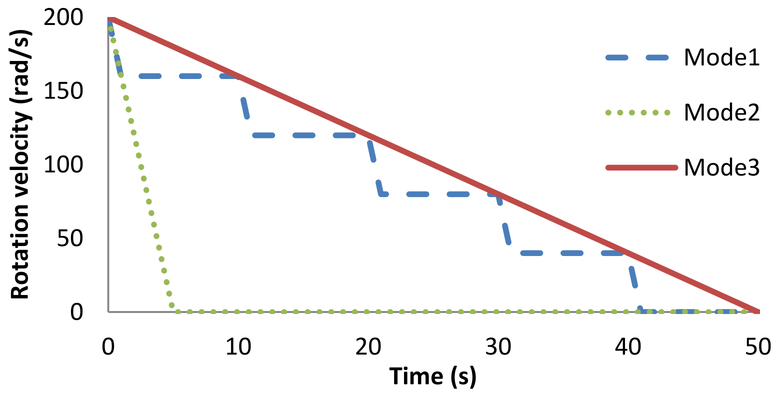

Figure 9 Velocity/time courses comparison for the three brake application modes

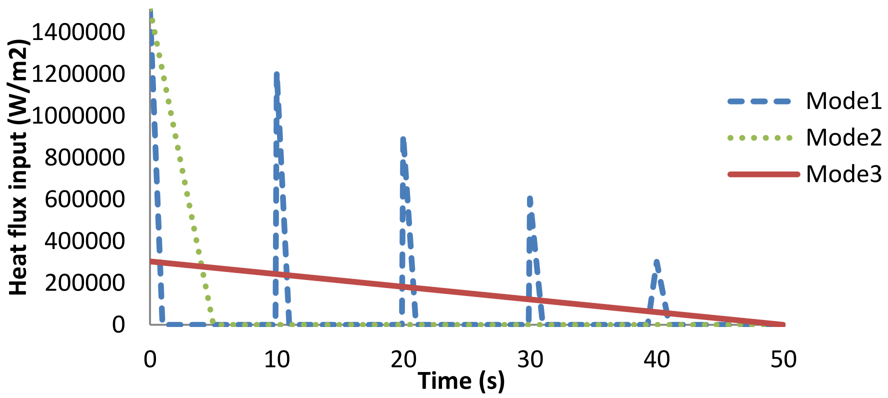

Figure 10 Heat flux input comparison for the three brake application modes

The temperature evolution characteristics for three types of brake application were investigated. The vehicle speed/time data are represented by figure 9. It can be seen that for the braking mode 1, there are five identical cycles. Each of the cycle has one second braking process and nine seconds constant vehicle speed without heat generation. Thus this braking mode can be regarded as snub braking. Brake mode 2 is a single brake application with high deceleration which takes 5 seconds to stop the vehicle. The mode 3 is a slow single brake which takes 50 seconds to stop the vehicle and maintains consistent braking force (deceleration).

Figure 10 shows the heat flux input over time for each of the modes. According to equation 1, the generated heat flux of mode 1 shows a periodic decrease at each brake application due to the decrease of initial velocity. For mode 2 and mode 3, they have identical total heat input but different durations. Mode 1 and mode 2 have same braking force whereas mode 2 and mode 3 have the same total heat flux.

The maximum disc surface temperature results are shown in figure 11. For the first two modes, it can be seen that the co-simulation results and the heat insulation results were similar at the beginning. The reason is that the heat conduction and convection cannot dissipate the huge amount of heat inputted in a short time. However, it can be seen that the temperature difference at the 3rd brake application was 23 ℃ which implies that the contribution of cooling has emerged. Regarding the braking mode 3, there is not sharp variation on the curves. Thus this result illustrated that there is not a rapid heat generation period under low deceleration but that cooling is significant over longer durations.

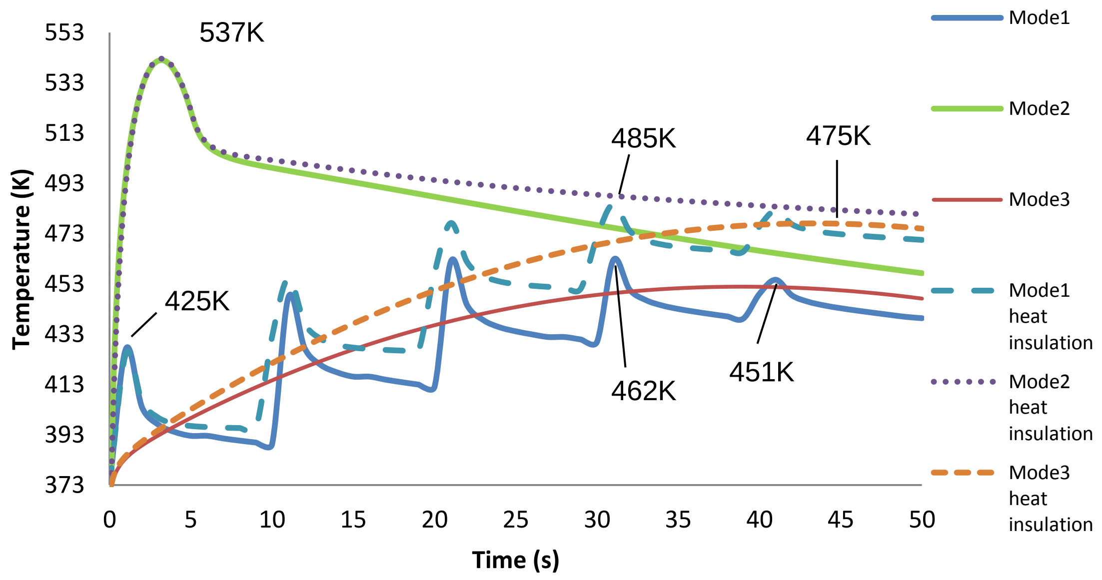

Figure 11 Temperature evolution time courses comparison

Two important observations are obtained from the 50s braking operations for the three modes: Firstly, under the adiabatic condition, it can be seen that the difference in final temperature between mode 1 and mode 2 was approximately 10 ℃, whilst mode 3 had only approximately 5 ℃ temperature difference when compared with mode 1 and mode 2. These observations mean that, due to similar amount of heat input, the terminal temperatures for the three modes are very close for adiabatic models. Secondly, for the temperature difference between adiabatic and co-simulation condition, mode 3 shows the largest difference (33 ℃), whilst 31 ℃ in mode 1, and 23 ℃ in mode 2. This indicated that the cooling effect of mode 1 and 3 are close and greater than mode 2. It implies that the cooling effects show good correlation with the vehicle velocity which is a significant advantage of the co-simulation in terms of cooling effect prediction.

5 CONCLUSION

In this study, a transient conjugate heat transfer co-simulation disc brake model has been performed. Through a parameter study for different mesh density, disc material, disc geometric construction, and braking applications, the following conclusion can be made under the conditions of this study:

- The co-simulation model is not particularly sensitive to the mesh density of the CFD model.
- The coupling of two codes does not increase the computational time.
- The disc material can affect the temperature distribution through thickness.
- The ventilated disc shows its advantages in cooling performance by 145% of the solid disc.

In summary, the result of this study demonstrated the good capability and feasibility of conjugate heat transfer co-simulation in brake system thermal analysis. The co-simulation has the capability to predict the heat transfer especially in complex transient braking application. It is believed that with the increasing requirement of brake system thermal performance, the conjugate heat transfer method is an appropriate approach for design improvement.

ACKNOWLEDGMENT

The authors would like to appreciate the support from Fraunhofer SCAI.

REFERENCE

(1) Limpert, R., “Analysis and design of automotive brake systems”, Society of Automotive Engineers, ISBN 1560912618, 1992

(2) Pevec, M., Lerher, T., Potrc, I. and Vranesevic, D., “Numerical temperature analysis of brake disc considering cooling”, Advance Engineering, 4(1), pp. 55-64, 2010

(3) Belhocine, A. and Bouchetara, M., “Thermal Analysis of a Solid Brake Disc”, Applied Thermal Engineering, 2012(32), pp. 59-67, 2012Tang

(4) Tang, J.H. and Qi, H.S., “FEM And CFD Co-simulation Study of a Ventilated Disc Brake Heat Transfer”, EuroBrake, Dresden, June 2013

(5) http://www.russellductile.co.uk/node/13

(6) Galindo-Lopez, C.H. and Tirovic, M., “Understanding and improving the convective cooling of brake discs with radial vanes”, Proceedings of the Institution of Mechanical Engineers, Part D: Journal of Automobile engineering, vol. 222(7), pp. 1211-1229, 2008